Molecular Weight-Dependent Behavior of the Twist Distortion in a Nematic Monodomain Containing a Main-Chain Liquid Crystal Polymer

Fu-Lung Chen and A. M. Jamieson*

Department of Macromolecular Science, Case Western Reserve University, Cleveland, Ohio 44106

*Received October 12, 1993; Revised Manuscript Received January 4, 1994**

ABSTRACT: The twist viscoelastic coefficients of dilute nematic solutions in 4′-(pentyloxy)-4-cyanobiphenyl (5OCB) of a main-chain liquid crystal polymer, TPB-10, which has a mesogenic group, 1-(4-hydroxy-4′-biphenylyl)-2-(4-hydroxyphenyl)butane, separated by flexible decamethylene spacers, were determined over a wide range of molecular weight using electric field-dependent dynamic light scattering. A Mark–Houwink–Sakurada relationship $[\eta] = KM_v^a$ was found for the intrinsic twist viscosity, with different exponents for oligomeric and polymeric chains. The oligomer behavior is interpreted as comparable to that of a free-draining rigid rod, while the polymer chains appear to approach the free-draining random coil limit. By invoking the wormlike chain model, the chain persistence length is determined. In addition, the configurational anisotropies of the polymers can be estimated. The apparent axial ratio of the chain decreases with molecular weight and then becomes constant. The results are thus consistent with the theoretical prediction for the crossover from rigid rod to a biased random coil. Finally, a model calculation for the dimer, trimer, and tetramer leads to an estimate of the probability of a hairpin turn per repeat unit.

Introduction

Main-chain nematic liquid crystal polymers (LCP) have a very different configurational and viscoelastic behavior in the nematic state from that in the isotropic state, because the nematic field has a strong effect on the internal molecular degrees of freedom. Thus, when a LCP is dissolved in a low molar mass nematogen (LMMN), the anisotropic shape of the LCP chain is determined by the competition between the three-dimensional entropic expansion and the tendency of the mesogenic groups to be aligned with the nematic field. The anisotropic radii of gyration, $R_\parallel$ and $R_\perp$, of the polymer chain in nematic solvents have been determined by small-angle X-ray scattering[1] and small-angle neutron scattering (SANS).[2] Here, $\parallel$ and $\perp$ refer to measurements parallel and perpendicular, respectively, to the nematic director, i.e., to a unit vector oriented along the average nematic axis. In addition, the viscoelastic properties of a nematic monodomain containing a LCP dissolved in a LMMN are expected to be a sensitive function of the molecular architecture. Such properties have been intensively studied recently.[3–14] The elastic constants and viscosity coefficients which characterize the splay, twist, and bend distortions of the nematic solution can be determined via the associated Freedericksz transition characteristics under magnetic or electric fields[15,16] and by static and dynamic light scattering measurements.[3,17–19] Finally, a theoretical model has been developed by Brochard[20] which provides expressions for certain viscosity increments as a function of $R_\parallel$ and $R_\perp$.

Of particular interest to us in the following study is the possibility, pointed out in a recent theoretical model of chain configuration in the nematic state,[21] that a main-chain LCP may exhibit behavior ranging from rodlike to random-coil statistics depending upon the ratio of the persistence length to the chain contour length even in a strong nematic field. To gain insight into the chain statistics, the relationship between the molecular weight and radii of gyration or the viscosity increments must be obtained for LCPs of narrow polydispersity. Comparatively few investigations concerning such relationships have been previously reported.[8,9] In one study, Pashkovskii and Litvina[8] reported that, based on measurements of the twist viscosity increment, poly[(decamethylenefumaroyl)bis(4-oxybenzoate)] behaves as a nondraining random coil, while poly[(3,3′-biphenylenesuberoyl)bis(4-oxybenzoate)] behaves as a free-draining random coil; from similar studies, Gu et al.[9] found that the main-chain LCP TPB-X (X = 5, 7, 9, 11) is intermediate between a free-draining random coil and a free-draining fully-extended rigid rod. We note, however, that polydisperse polymer specimens were used in all of these investigations. In this paper, we seek to determine the molecular weight dependence of the intrinsic twist viscosity using monodisperse TPB-10 oligomers and polymers of narrow polydispersity. The data are interpreted to yield the persistence length of this main-chain LCP and estimates of the chain anisotropy $R_\parallel/R_\perp$ for the polymer fractions.

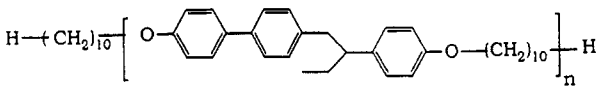

Figure 1. Chemical structure of TPB-10: A racemic mixture of this species was utilized in our investigation.

Experimental Section

A. Materials. The main-chain LCP TPB-10 consists of a mesogenic unit, 1-(4-hydroxy-4′-biphenylyl)-2-(4-hydroxyphenyl)butane, separated by flexible decamethylene spacers. Specimens of this main-chain LCP were supplied to us by Prof. Virgil Percec, Case Western Reverse University. The chemical structure, molecular weights, and chain contour lengths are listed[22] in Figure 1 and Table 1. It is important to recognize that since the true molecular weights of oligomers are different[22] from the GPC-determined values, relative to polystyrene standards, by a nearly constant ratio, we use this ratio to obtain true molecular weights for the polymeric species from their GPC molecular weights. It is the corrected values which were further used to calculate the chain contour lengths. 4′-(Pentyloxy)-4-biphenylcarbonitrile (5OCB, T_{NI} = 67 °C), previously shown[23] to be a LMMN solvent for TPB-10, was obtained from Aldrich Chemical Co. All materials were used as received without further purification. Planar (homogeneous) monodomains, in which the

* Abstract published in *Advance ACS Abstracts*, March 1, 1994.

0024-9297/94/2227-1943$04.50/0

Table 1. Molecular Weights and Chain Contour Lengths of TPB-10 Oligomers and Polymers

	monomer	dimer	trimer	tetramer	no. 5	no. 6	no. 7	no. 8	no. 9
M_c[a]	598	1054	1510	1966					
$M_{w,GPC}$[b]	960	1670	2420	3070	13330	17300	25080	45820	75440
M_w/M_n[b]	1.0	1.0	1.0	1.0	1.18	1.21	1.20	1.28	1.34
$M_{w,a}$[c]	598	1054	1510	1966	8440	10950	15860	28990	47730
L_w[d] (Å)	47.6	81.5	115.4	149.3	629.9	816.6	1181.5	2156.6	3548.5

[a] Calculated molecular weight. [b] Determined by GPC using chloroform as a solvent and polystyrene as a standard.[22] [c] Actual molecular weight obtained by correcting $M_{w,GPC}$ via the ratio between $M_{w,GPC}$ and M_c of oligomers. [d] Chain contour length based on $M_{w,a}$.

average molecular direction is parallel to the glass surfaces, were prepared using rubbed polyimide-coated conductive glass slides graciously supplied to us by Mr. Pat Dunn at Kent State University, Kent, OH. Homeotropic monodomains, where the average molecular direction is perpendicular to the glass surfaces, were prepared using conductive glass slides coated with lecithin (Epikuron, Lucas Meyer Inc.). The sample cell thickness was measured by interferometry[24] with an experimental error of 1%. The spacer used in the cell was 25-μm Mylar, and the cells were sealed with epoxy (Devcon). Cells were filled with nematic mixtures at a temperature around 65 °C. A Carl Zeiss optical polarizing microscope equipped with a Mettler FP82HT hot stage and a Mettler FP90 central processor was used to evaluate the nematic alignment, based on the fact that, under cross polarizers, homeotropic alignment and disclinations in planar alignment appear dark. This method was also used to determine the nematic to isotropic transition temperatures, T_{NI}, of the samples at a heating rate of 0.2 °C/min. The T_{NI} of the mixtures, measured as the lower bound of the transition zone, was very close to that of pure 5OCB.

B. Electric Field-Dependent Dynamic Light Scattering. A detailed description of the methods and analytical procedures for the application of dynamic light scattering to the determination of viscoelastic parameters of nematic liquid crystals can be found elsewhere.[3,17-19] We performed light scattering measurements in the homodyne configuration, using a photon correlation spectrometer equipped with a 6-mW He–Ne linearly polarized laser and a BI-2030AT 264-channel digital correlator. The sample cell was positioned in a refractive index-matching bath containing 4-*tert*-butyltoluene. The sample cell temperature was controlled by a circulating bath at 52.0 ± 0.1 °C. In the light scattering experiments, the director, i.e., the average molecular direction of a homeotropic monodomain is oriented perpendicular to the incident polarization and parallel to the incident wave vector. The decay rate, Γ_2, in the presence of an electric field parallel to the director can be expressed as[25]

$$\Gamma_2 = (K_{33}q_\parallel^2 + K_{22}q_\perp^2)/\eta_2 + \epsilon_0\Delta\epsilon V^2/(d^2\eta_2) \quad (1a)$$

$$\eta_2 = \gamma_1 - [(\eta_a/\alpha_2^2)q_\perp^2/q_\parallel^2 + \eta_c/\alpha_2^2]^{-1} \quad (1b)$$

$$q_\parallel = 2\pi(n_\perp - n\cos\theta)/\lambda_0 \quad (1c)$$

and

$$q_\perp = (2n\pi\sin\theta)/\lambda_0 \quad (1d)$$

where K_{22} and K_{33} are the twist and bend elastic constants, respectively; λ_0 is the wavelength of incident light in vacuum (632.8nm); n and $n_\perp$ are respectively the effective and ordinary refractive indices of nematic mixtures; θ is the scattering angle in the nematic mixture and can be calculated by Snell's law, viz., $n\sin\theta = n_m\sin\theta_{lab}$, where n_m is the refractive index of the matching liquid and θ_{lab} is the scattering angle in the laboratory frame, i.e., the angle between the transmitted laser beam and the photomultiplier tube; γ_1 is the twist viscosity; α_2 refers to a Leslie viscosity;[26] η_a and η_c are Miesowicz viscosities;[27] V is the applied voltage across the cell; d is the thickness of the cell; ϵ_0 is the dielectric permittivity in vacuum; and $\Delta\epsilon$ is the dielectric anisotropy of the liquid crystal solution. The dielectric anisotropy is obtained by measuring the capacitance of the sample cell while an increasing bias voltage is applied to a planar monodomain.[10] The frequencies of the bias voltage and probe signal were 50 and 6000 Hz, respectively. Note that the T_{NI} of the planar cells is usually slightly different from those of the homeotropic cells ($\Delta T_{NI} \leq 1.0$ °C), which is probably due to the dissolution of trace amounts of lecithin in the latter. To minimize errors from this source, the measurements of $\Delta\epsilon$ were always performed at $\Delta T = T_{NI} - T = 15$ °C. In electric field-dependent dynamic light scattering measurements, the applied field frequency was also 6000 Hz.

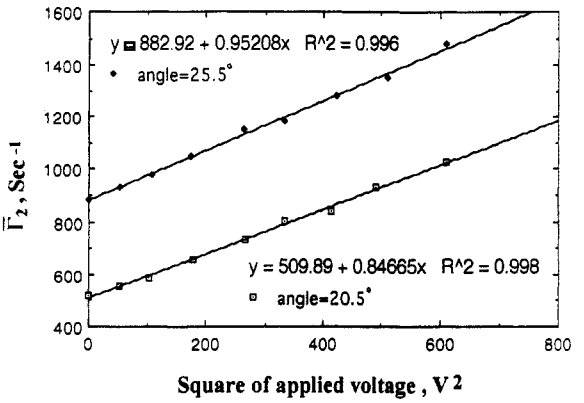

Figure 2. Dependence of the average decay rate on the applied voltage for dynamic light scattering from 0.477 wt % TPB-10 no. 9 in 5OCB at 52 °C.

From eq 1, we know that we can measure the pure twist mode if $(\eta_a/\alpha_2^2)q_\perp^2/q_\parallel^2$ is very large. However, since the magnitude of η_a/α_2^2 for our samples is generally very small, the angle at which we can measure the pure twist mode is also very small. It is difficult to perform the light scattering measurements at such small angles due to the flare from the glass surface. We therefore performed measurements at several different angles for each sample and determined K_{22} and γ_1 via fits to eq 1.

Results and Discussion

To confirm the validity of eq 1, the average decay rates ($\bar{\Gamma}_2$) vs V^2 at two different angles for 0.477 wt % TPB-10 no. 9 (M_w = 47730) in 5OCB are presented in Figure 2. As evident from this figure, the linearity of the plot of $\bar{\Gamma}_2$ vs V^2 is excellent and the slope increases with angle as expected. In principle, we can obtain K_{22}, K_{33}, γ_1, η_a/α_2^2, and η_c/α_2^2 by performing field-dependent light scattering measurements at different angles and generating fits to eq 1. However, since we can accurately measure decay rates only in the range 15–50°, the weighting in the curve fitting for K_{33}, η_a/α_2^2, and η_c/α_2^2 is not sensitive enough to obtain reliable results. Therefore, we present only data on K_{22} and γ_1 in this paper.

Table 2 displays the twist elastic constants of the nematic mixtures as well as that of pure 5OCB. As observed from this table, the twist elastic constants of mixtures are always slightly higher than that of pure 5OCB. This situation is quite different from that encountered in mixtures containing side-chain liquid crystal polymers, where the twist elastic constant is usually decreased relative to the nematic solvent.[3,10,12] This result is consistent with previous studies which indicate that the splay and bend elastic constants increase on addition of main-chain LCP.[5,6,11,14] Figure 3 shows η_2 at various scattering angles in the laboratory frame, together with the least squares fits to eq 1b, for pure 5OCB and a 1.34 wt % solution of TPB-10 no. 7 (M_w = 15860) in 5OCB. As seen in Figure 3b, it is clear that

Table 2. Twist Elastic Constants of Pure 5OCB and TPB-10/5OCB Solutions at 52.0 °C

	5OCB	dimer (9.99%)	trimer (6.71%)	tetramer (5.01%)	no. 5 (1.56%)	no. 6 (1.56%)	no. 7 (1.34%)	no. 8 (0.99%)
$K_{22} \pm 5\%$ (10^{-8} dyn)	32.9	35.4	33.9	34.1	34.9	34.9	36.1	36.4

	no. 9 (0.478%)	no. 9 (0.92%)	no. 9 (1.50%)	monomer/tetramer (1:1, 5.99%)	dimer/tetramer (1:1, 5.63%)
$K_{22} \pm 5\%$ (10^{-8} dyn)	34.8	34.7	35.0	35.0	36.1

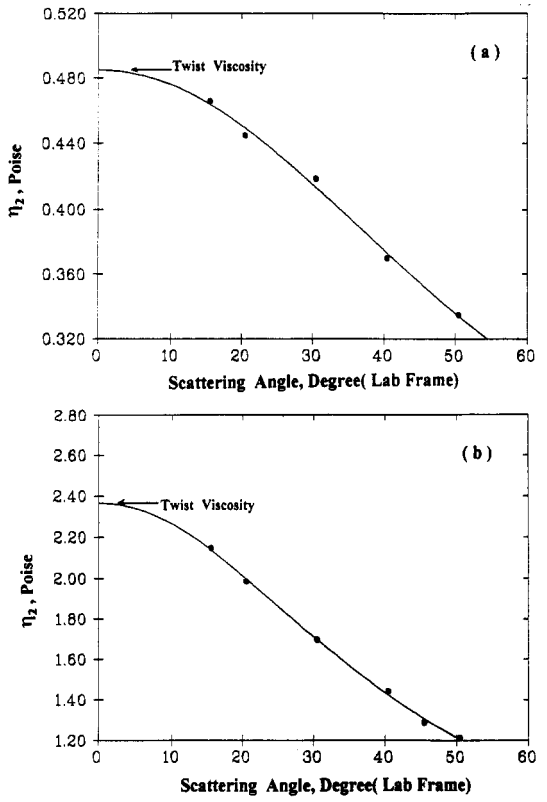

Figure 3. Dependence of the viscosity coefficient η_2 upon scattering angle in the laboratory frame: (a) pure 5OCB; (b) 1.344 wt % TPB-10 no. 7 in 5OCB at 52 °C. The solid lines are the best fit to eq 1b.

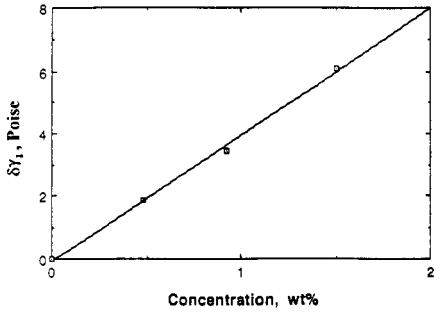

Figure 4. Dependence of the twist viscosity increment on polymer concentration for TPB-10 no. 9 in 5OCB at 52 °C.

for this polymer solution, even at 10° (laboratory frame), the difference between η_2 and γ_1 is around 5% due to the fact that the ratio of η_a to α_2^2 is very small.

To ensure that the viscoelastic properties we measured are within the linear concentration regime (i.e., within a range where the viscous contributions of dissolved chains are linearly additive), we measured the concentration dependence of the twist viscosity increment for the polymer with highest molecular weight, TPB-10 no. 9. The results are shown in Figure 4. Clearly, the twist viscosity increases linearly with concentration of added polymer up to a concentration of $C = 1.5\%$. Within this concentration range we can define a unique value of the intrinsic twist viscosity, $[\gamma_1] = \delta\gamma_1/C\gamma_1°$, where the viscosity increment $\delta\gamma_1 = \gamma_1 - \gamma_1°$ and γ_1 and $\gamma_1°$ are the viscosities of solution and solvent, respectively. For TPB-10 no. 9, we determine $[\gamma_1] = 809$ g/g and therefore deduce that linear additivity of the twist viscosity holds for this polymer in 5OCB in the concentration range $C[\gamma_1] \leq 12.1$. For the other mixtures, we assume this criterion also applies to ensure that our measurements are well within the linear concentration regime, as shown in Table 3.

Table 3. Intrinsic Twist Viscosities and Experimental Concentrations of TPB-10/5OCB Solutions

	no. 9	no. 8	no. 7	no. 6	no. 5	tetramer	trimer	dimer
$[\gamma_1]$ (g/g)	809	494	287	208	157	41.3	27.5	15.8
C (wt %)[a]	≤1.5	0.99	1.34	1.56	1.56	5.01	6.71	9.99
$C[\gamma_1]$	≤12.1	4.89	3.85	3.24	2.45	2.07	1.85	1.58

[a] Concentration used in this investigation.

As mentioned earlier, to obtain insight into the LCP chain statistics in solution in low molar mass nematogens, it is of interest to determine the molecular weight dependence of the twist viscosity of the solution. The dependence of the intrinsic twist viscosity on the LCP chain contour length is shown in Figure 5. Note that we utilize the weight-average chain contour length for reasons we will discuss later. The most interesting aspect of Figure 5 is that the oligomers and polymers have different dependences of the intrinsic twist viscosity on the chain contour length. By least squares fits, the chain contour length dependences of the intrinsic twist viscosity are found to be, for the oligomers

$$[\gamma_1] = 0.0146L^{1.59} \tag{2a}$$

and, for the polymers

$$[\gamma_1] = 0.387L_w^{0.93} \tag{2b}$$

Before proceeding to a discussion of the implication of eqs 2a and 2b for the chain configuration and hydrodynamic behavior, it seems appropriate to decide which molecular weight average should applied to the intrinsic twist viscosity of a polydisperse LCP in nematic solution. As is well known in isotropic solution, for a polydisperse polymer

$$[\eta] = KM_v^{\alpha} \tag{3a}$$

where

$$M_v = (\sum n_i m_i^{\alpha+1}/\sum n_i m_i)^{1/\alpha} \tag{3b}$$

To establish whether eq 3 remains valid for the twist viscosity, we measured the intrinsic twist viscosities of nematic solutions of two mixtures, a 1:1 monomer/tetramer mixture and a 1:1 dimer/tetramer mixture, both in 5OCB. The viscosity-average (L_v) and weight-average (L_w) chain contour lengths, their corresponding predicted intrinsic twist viscosities, and the observed results can be found in Table 4. Table 4 tells us that the experimental intrinsic twist viscosity is numerically consistent with the value predicted based on the viscosity-average chain contour length, within the experimental error (~4%). In other words, eq 3 holds for the twist viscosity of nematic polymer

Table 4. Predicted and Observed Intrinsic Twist Viscosities of 1:1 Monomer/Tetramer and 1:1 Dimer/Tetramer Mixtures in 5OCB

polymer mixture	L_v (Å)	$[\gamma_1]_{v,p}$ (g/g)[a]	L_w (Å)	$[\gamma_1]_{w,p}$ (g/g)[b]	$[\gamma_1]$ (g/g)[c]
monomer/tetramer	99.02	21.53	91.12	18.87	21.85
dimer/tetramer (1:1)	118.0	28.45	115.08	27.33	28.30

[a] Predicted intrinsic twist viscosity based on viscosity-average chain contour length (L_v). [b] Predicted intrinsic twist viscosity based on weight-average chain contour length (L_w). [c] Observed intrinsic twist viscosity.

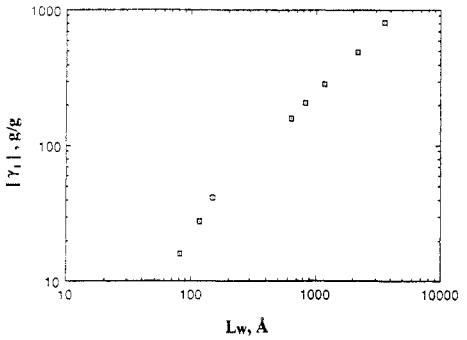

Figure 5. Dependence of the intrinsic twist viscosity on chain contour length of TPB-10 in 5OCB at 52 °C.

solutions. Note that this result provides additional confirmation that the concentrations utilized are within the linearly additive viscosity regime. For our polymer specimens, since the exponent α in eq 3 is close to unity and since the polydispersity is quite narrow, L_w is nearly identical to L_v, and, hence, we use L_w when comparing the data for the polymers versus that of the oligomers.

To discuss the experimental results in terms of the molecular chain configuration and hydrodynamic behavior, we first recall the theoretical prediction of Brochard:[20]

$$\delta\gamma_1 = (CN_A/M)[\lambda_\parallel\lambda_\perp R_\parallel{}^2R_\perp{}^2/(\lambda_\parallel R_\parallel{}^2 + \lambda_\perp R_\perp{}^2)](R_\parallel{}^2 - R_\perp{}^2)^2/(R_\parallel{}^2R_\perp{}^2) \quad (4)$$

where C is the polymer concentration in g/mL; N_A is Avogadro's number; M is the molecular weight of the polymer; $\lambda_\parallel$ and $\lambda_\perp$ are respectively the friction coefficients associated with motions parallel and perpendicular to the director; and $R_\parallel$ and $R_\perp$ are the radii of gyration parallel and perpendicular to the director, respectively.

Assuming a free-draining condition to be valid for the oligomers and for the highly extended polymer chains, we may write $\lambda_\parallel = LZ_\parallel$ and $\lambda_\perp = LZ_\perp$,[20] where $Z_\parallel$ and $Z_\perp$ are the unit length friction coefficients in the two orthogonal directions. If we set $R_\perp = xR_\parallel$, then, from eq 4,

$$\delta\gamma_1/C \propto Z_\parallel Z_\perp R_\parallel{}^2(1-x^2)^2/(Z_\parallel + Z_\perp x^2) \quad (5)$$

For a rigid rod, $x^2 \approx 0$ and $R_\parallel \propto L$,[21] we have

$$\delta\gamma_1/C \propto L^2 \quad (6)$$

For a random coil biased along the nematic director, $R_\parallel \propto L^{0.5}$ and x is independent of L;[21] therefore

$$\delta\gamma_1/C \propto L \quad (7)$$

If a nondraining condition exists, i.e., if there are strong hydrodynamic interactions between the LCP chain segments, we write[20] $\lambda_\parallel \propto Z_\parallel R_\parallel$ and $\lambda_\perp \propto Z_\perp R_\perp$. Thus, since $R_\perp = xR_\parallel$, it follows that

$$\delta\gamma_1/C \propto Z_\parallel Z_\perp x(1-x^2)^2R_\parallel{}^3/[M(Z_\perp x^3 + Z_\parallel)] \quad (8)$$

where $Z_\parallel$ and $Z_\perp$ are now the unit length friction coefficients associated with the motion of an impenetrable ellipsoid whose longer axis is parallel to the nematic director. For a biased random coil chain, x is constant and $R_\parallel \propto L^{0.5}$;[21] therefore

$$\delta\gamma_1/C \propto L^{0.5} \quad (9)$$

Experimentally, we found $\delta\gamma_1/C \propto L^{1.59}$ for the oligomers and $\delta\gamma_1/C \propto L_w{}^{0.93}$ for the polymers. This suggests to us that the oligomers exhibit hydrodynamic behavior rather close to that of a free-draining rigid rod and that the corresponding behavior of the polymers is nearly that of a free-draining random coil. To obtain a more quantitative description of the configurational behavior, we can estimate the persistence length of this LCP by employing the wormlike chain model for a semirigid molecule.[28] In the isotropic state, the wormlike coil model yields the following expression for the mean-square radius of gyration:

$$\langle R^2\rangle = a^2[L/(3a) - 1 + 2a/L - (2a^2/L^2)(1 - \exp(-L/a))] \quad (10)$$

where a is the persistence length and L is the contour length of the chain. In the nematic environment, the end-to-end distance in the direction parallel to the director can be expressed by[21]

$$\langle r_\parallel{}^2\rangle = (2/3)La[1 - (a/L)(1 - \exp(-L/a))](9/4)f(\Delta) \quad (11)$$

where the term $(9/4)f(\Delta)$ is an increasing function of the nematic potential and has a value of unity when the nematic potential equals zero. Thus, it follows that[28] $R_\parallel$ can be written as

$$\langle R_\parallel{}^2\rangle = (a^2/3)[L/(3a) - 1 + 2a/L - (2a^2/L^2)(1 - \exp(-L/a))](9/4)f(\Delta) \quad (12)$$

Note that in eq 12 the persistence length, a, is also a function of the nematic field.

Our experiments were performed at equal reduced temperatures, i.e., at equivalent nematic field potentials. Hence $f(\Delta)$ and the persistence length are constants. Therefore, we may write the following expression for a normalized $\langle R_\parallel{}^2\rangle$:

$$\frac{\langle R_\parallel{}^2\rangle}{\langle R_\parallel{}^2\rangle_r} = \frac{(L/(3a)) - 1 + (2a/L) - (2a^2/L^2)(1 - \exp(-L/a))}{(L_r/(3a)) - 1 + (2a/L_r) - (2a^2/L_r{}^2)(1 - \exp(-L_r/a))} \quad (13)$$

where the subscript r refers to the reference molecular weight. For the oligomers, recalling that $\delta\gamma_1/C \propto L^{1.59}$, we deduce that the chain is well extended and we can safely assume that $x^2 \ll 1$. Consequently, from eq 5, we have

$$\frac{\delta\gamma_1/C}{(\delta\gamma_1/C)_{dimer}} = \frac{R_\parallel{}^2}{(R_\parallel{}^2)_{dimer}} \quad (14)$$

where the dimer is used as the reference chain. This relationship (eq 14) enables us to estimate the persistence length via an equal-weight least-squares curve fitting of

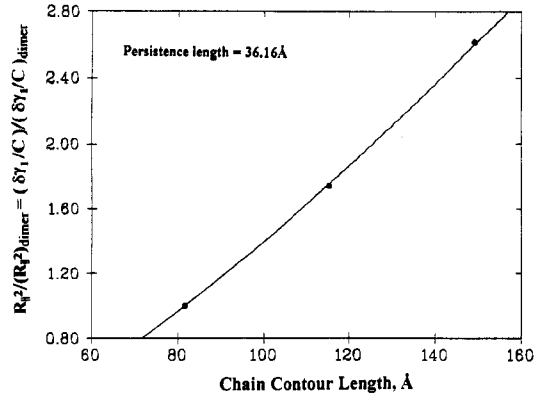

Figure 6. Dependence upon chain contour length of $R_\parallel^2/(R_\parallel^2)_{dimer}$ for TPB-10 oligomers in 5OCB. The solid line is the best fit to eq 13 and yields the persistence length a = 36.16 Å.

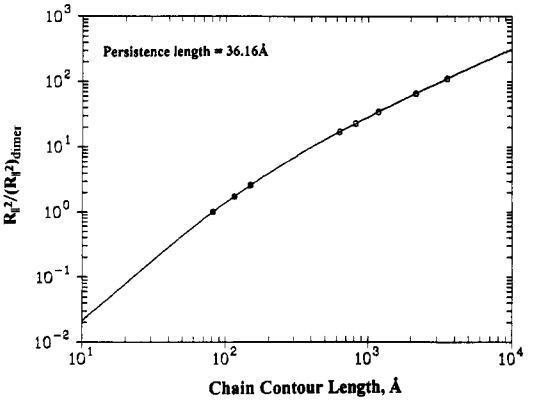

Figure 7. Simulated variation of $R_\parallel^2/(R_\parallel^2)_{dimer}$ of TPB-10 with chain contour length via eq 13 using a persistence length a = 36.16 Å. The filled circles are the experimental oligomer data, while the open circles are the values used to calculate the chain anisotropies of polymer species shown in Table V.

the oligomer data to eq 13, as shown in Figure 6. Recognizing that we have only two data points in addition to the reference point in this analysis, we nevertheless believe that the derived persistence length a = 36.16 Å is reliable, in view of the fact that there is only one adjustable fit parameter, i.e., the persistence length. Note that our value for the persistence length is slightly larger than the contour length of one fully-extended repeat unit, viz., 33.87 Å.

We cannot apply eq 14 to the high polymers since we expect the approximation $x^2 \ll 1$ to fail at these molecular weights. To see this, we use the obtained persistence length and simulate via eq 13 in Figure 7 the contour length dependence of the normalized $R_\parallel^2$. Clearly, the predicted values for our polymer species, shown as open circles, fall beyond the crossover to a biased random coil. This is approximately consistent with our above deduction, based on the experimental observation $\delta\gamma_1/C \propto L_w^{0.93}$, that the hydrodynamic behavior of the polymer chains is that of a free-draining unperturbed random coil, for which we expect $\delta\gamma_1/C \propto L_w^{1.0}$.

From Figure 7, it is therefore not surprising that a self-consistent fit cannot be obtained for both oligomers and polymers via eqs 13 and 14 since the latter assumes the rigid rod limit, $x^2 \ll 1$. To achieve a self-consistent analysis, we need to consider the effect of finite x^2 in eq 5 for the polymer chains. For free-draining coils, it appears reasonable to assume, for the unit length frictional coefficients, that $Z_\parallel \approx Z_\perp$, and hence, for the polymers, we may write

$$\frac{\delta\gamma_1/C}{(\delta\gamma_1/C)_{dimer}} = \frac{(1-x^2)^2}{(x^2+1)}\frac{R_\parallel^2}{(R_\parallel^2)_{dimer}} \qquad (15)$$

Table 5. Chain Anisotropies $R_\parallel/R_\perp$ of TPB-10 Polymers in 5OCB

specimen	L_w (Å)	$(\delta\gamma_1/C)/(\delta\gamma_1/C)_{dimer}$	$R_\parallel^2/(R_\parallel^2)_{dimer}$	$R_\parallel/R_\perp$
no. 5	629.9	9.95	17.16	2.39
no. 6	816.6	13.15	23.09	2.36
no. 7	1181.5	18.17	34.75	2.20
no. 8	2156.6	31.24	66.05	2.06
no. 9	3548.5	51.22	110.81	2.03

Note that the left-hand side of this equation is known experimentally and that the ratio $R_\parallel^2/(R_\parallel^2)_{dimer}$ is available from the wormlike coil model, i.e., eq 13, with a = 36.16 Å, as also shown in Figure 7. Therefore, the chain anisotropy, $R_\parallel/R_\perp$, can be estimated from eq 15. The results are displayed in Table 5, which shows that the chain anisotropy $R_\parallel/R_\perp$ is not very large and decreases slowly with molecular weight, reaching a constant minimum value near 2.0. These observations are consistent with a crossover from a rigid rod to a biased random coil. For a rigid rod, $R_\parallel/R_\perp$ will increase with molecular weight. However, sufficiently long chains are expected to follow a biased random coil. Therefore the $R_\parallel/R_\perp$ of polymers, falling beyond the crossover to a biased random coil, should decrease with molecular weight to a constant minimum value.[21] As a quantitative comparison of the limiting chain anisotropy of the polymers with existing theory, we consider the nematic Kuhn chain model,[29] which gives

$$R_\parallel^2/R_\perp^2 = (1+2S)/(1-S) \qquad (16)$$

Here S is the nematic order parameter, which is defined as $0.5\langle 3\cos^2\phi - 1\rangle$, where ϕ is the angle between the axis of an individual molecule and the director and the angular brackets indicate a configurational average. For TPB-10 in 5OCB, we do not know the precise order parameter. However, to an approximation, we know[30] that the elastic constants $K_{ii} \sim S^2$. Experimentally, we find that the twist elastic constants of the mixtures on average increase over that of pure 5OCB by only ~6%, implying the order parameter increases only ~3%, which is not significant. Therefore, it is reasonable to assume the order parameter of the polymer is equal to that of pure 5OCB at $T_{NI} - T$ = 15 °C, which is approximately 0.54.[31] Inserting this value in eq 16 leads to a predicted chain anisotropy $R_\parallel/R_\perp$ = 2.13. Clearly, this theoretical value is numerically consistent with that, $R_\parallel/R_\perp$ = 2.03, estimated from the experimental data (Table 5) via the wormlike chain model. We note further that the chain anisotropy estimated here is comparable to those reported by Pashkovsky and Litvina[6] and by Mattoussi and Veyssie[5] for different main-chain LCPs dissolved in LMMNs but rather smaller than that reported via SANS measurements by D'Allest et al.[2] Note, however, that as predicted by eq 16 the chain anisotropy can vary substantially with the nematic order parameter.

Finally, we recognize that it is of interest to attempt a more microscopic analysis of the configurational states present in the oligomer solutions. To achieve this, we model the oligomer solutions as mixtures of configurational isomers containing either no hairpin turns or a single hairpin turn. The configurational isomeric states of dimer, trimer, and tetramer can then be represented as shown in Figure 8, where the statistical weight fractions, w_i, of each configuration are represented as a function of P, the probability of a hairpin turn per repeat unit. We also show L_i, the effective chain contour length contributing to the intrinsic twist viscosity. Assuming eq 6 is applicable to all configurational isomers, i.e., $[\gamma_1]_i \propto L_i^2$, and realizing that $[\gamma_1] = \sum W_i[\gamma_1]_i$, we have

$$[\gamma_1]_{dimer} \propto 81.5^2(1-P) + 40.75^2P \qquad (17a)$$

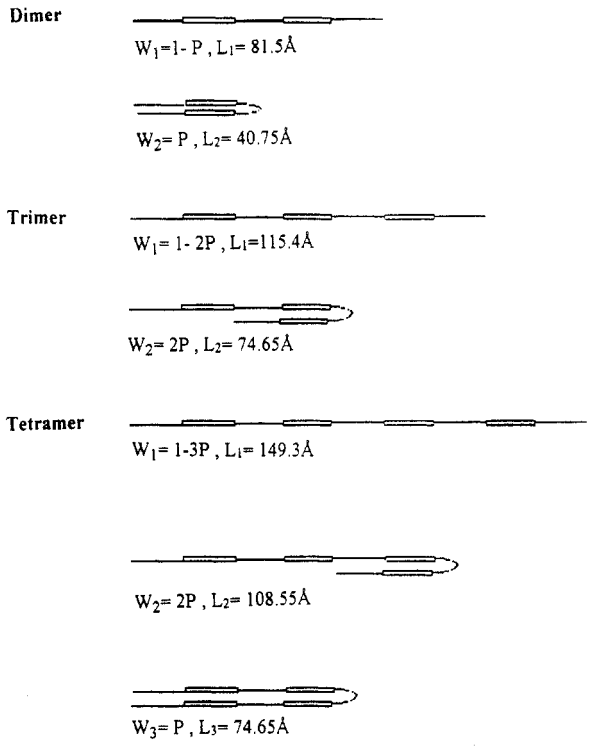

Figure 8. Configurational isomers of TPB-10 dimer, trimer, and tetramer in 5OCB: W_i is the statistical weight fraction, expressed in terms of P, the probability of one hairpin turn per repeat unit; L_i is the effective chain contour length contributing to the intrinsic twist viscosity.

Table 6. Probability P of One Hairpin Turn per Repeat Unit

$[\gamma_1]$ ratio	P
dimer/trimer = 0.575	0.26
dimer/tetramer = 0.383	0.20
trimer/tetramer = 0.666	0.16

$$[\gamma_1]_{\text{trimer}} \propto 115.4^2(1-2P) + 74.65^2 2P \qquad (17b)$$

and

$$[\gamma_1]_{\text{tetramer}} \propto 149.3^2(1-3P) + 108.55^2 2P + 74.65^2 P \qquad (17c)$$

Utilizing the experimental values of $[\gamma_1]$ for dimer, trimer, and tetramer, we can now determine the value of P from the experimental ratios $[\gamma_1]_{\text{dimer}}/[\gamma_1]_{\text{trimer}}$, $[\gamma_1]_{\text{dimer}}/[\gamma_1]_{\text{tetramer}}$, and $[\gamma_1]_{\text{trimer}}/[\gamma_1]_{\text{tetramer}}$. The results are listed in Table 6, which indicates the probability of one hairpin turn per repeat unit is $P = 0.21 \pm 0.05$. Such a small value of P confirms that it is reasonable to neglect configurational isomers with two hairpin turns in this analysis.

Conclusions

We have determined the molecular weight dependence of the intrinsic twist viscosity of a main-chain LCP, TPB-10, in a LMMN, 5OCB. We found that the traditional Mark–Houwink–Sakurada relationship, $[\eta] = KM_v^{\alpha}$, can be applied to the twist viscosity. From the large value of the exponent $\alpha = 1.59$, we infer that the oligomer chain behavior is close to that of a free-draining rigid rod; from the value $\alpha = 0.93$, we deduce that the polymer chain behaves approximately as a free-draining biased random coil. The persistence length of TPB-10 in 5OCB is determined to be $a = 36.16$ Å by curve fitting the oligomer data, close to the rigid rod limit, to the wormlike chain model. From the obtained persistence length and assuming a free-draining condition, the chain anisotropies of the polymers could be estimated and were found to decrease with molecular weight to a minimum asymptotic value. By modeling the oligomer solutions as mixtures of configurational isomers containing either no hairpin turns or one hairpin turn, we derive an estimate of the probability of a hairpin turn per repeat unit as ≈0.2. In future work, we hope to provide support for our conclusions by direct determination of the chain anisotropies via small-angle neutron scattering measurements.

Acknowledgment. We thank Prof. Virgil Percec at Case Western Reserve University for supplying the main-chain LCP. Also, we thank Mr. Pat Dunn at Kent State University for the courtesy of polyimide-coated glass slide. Finally, financial support from NSF Materials Research Group Award DMR 01845 is gratefully acknowledged.

References and Notes

(1) Mattoussi, H.; Ober, R. *Macromolecules* **1990**, *23*, 1809.
(2) D'Allest, J. F.; Sixou, P.; Blumstein, A.; Blumstein, R. B.; Teixeira, J.; Noirez, L. *Mol. Cryst. Liq. Cryst.* **1988**, *155*, 581.
(3) Gu, D.; Jamieson, A. M.; Rosenblatt, C.; Tomazos, D.; Lee, M.; Percec, V. *Macromolecules* **1991**, *24*, 2385.
(4) Weil, C.; Casagrande, C.; Veyssie, M. *J. Phys.* (*Fr.*) **1986**, *47*, 887.
(5) Mattoussi, H.; Veyssie, M. *J. Phys.* (*Fr.*) **1989**, *50*, 99.
(6) Pashkovsky, E. E.; Litvina, T. G. *J. Phys. II* (*Fr.*) **1992**, *2*, 521.
(7) Pashkovsky, E. E.; Litvina, T. G.; Kostromin, S. G.; Shibaev, V. P.; *J. Phys. II* (*Fr.*) **1992**, *2*, 1577.
(8) Pashkovskii, Ye. E.; Litvina, T. G. *J. Polym. Sci.* **1991**, *33*, 655.
(9) Gu, D.-F.; Jamieson, A. M.; Lee, M.-S.; Kawasumi, M.; Percec, V. *Liq. Cryst.* **1992**, *12*, 961.
(10) Gu, D.; Smith, S. R.; Jamieson, A. M.; Lee, M.; Percec, V. *J. Phys. II* (*Fr.*) **1993**, *3*, 937.
(11) Gilli, J. M.; Sixou, P.; Blumstein, A. *J. Polym. Sci., Polym. Lett. Ed.* **1985**, *23*, 379.
(12) Coles, H. J.; Sefton, M. S. *Mol. Cryst. Liq. Cryst. Lett.* **1985**, *1*, 159.
(13) Gu, D.; Jamieson, A. M.; Kawasumi, M.; Lee, M.; Percec, V. *Macromolecules* **1992**, *25*, 2152.
(14) Chen, F.-L.; Jamieson, A. M. *Macromolecules* **1993**, *26*, 6576.
(15) Brochard, F.; Pieranski, P.; Guyon, E. *J. Phys.* (*Fr.*) **1972**, *33*, 681; **1973**, *34*, 35.
(16) Brochard, F.; Pieranski, P.; Guyon, E. *Phys. Rev. Lett.* **1972**, *28*, 1681.
(17) Orsay Liquid Crystal Group. *J. Chem. Phys.* **1969**, *51*, 816.
(18) Orsay Liquid Crystal Group. *Phys. Rev. Lett.* **1969**, *22*, 1361.
(19) Sefton, M. S.; Bowdler, A. R.; Coles, H. J. *Mol. Cryst. Liq. Cryst.* **1985**, *129*, 1.
(20) Brochard, F. *J. Polym. Sci., Polym. Phys. Ed.* **1979**, *17*, 1367.
(21) Warner, M.; Gunn, J. M. F.; Baumgärtner, A. B. *J. Phys. A: Math. Gen.* **1985**, *18*, 3007.
(22) Kawasumi, M., Ph.D. Thesis, Department of Macromolecular Science, Case Western Reserve University, Cleveland, OH 44106, 1993.
(23) Chen, F.-L.; Jamieson, A. M. *Liq. Cryst.* **1993**, *15*, 171.
(24) Kinzer, D. Mol. Cryst. Liq. Cryst. Lett. **1985**, *1*, 147.
(25) Leslie, F. M.; Waters, C. M. *Mol. Cryst. Liq. Cryst.* **1985**, *123*, 101.
(26) Leslie, F. M. Q. *J. Mech. Appl. Math.* **1966**, *19*, 357.
(27) Miesowicz, M. *Bull. Int. Acad. Pol. Sci. Lett., Ser. A* **1936**, *28*, 228.
(28) Benoit, H.; Doty, P. *J. Phys. Chem.* **1953**, *57*, 958.
(29) Maffettone, P. L.; Marrucci, G. *J. Rheol.* **1992**, *36*, 1547.
(30) de Jeu, W. H. *Physical Properties of Liquid Crystalline Materials*; Gordon and Breach: London, 1980.
(31) Mitra, M.; Paul, R.; Paul, S. *Acta Phys. Pol.* **1990**, *A78*, 453.